Accurate calculations of phonon dispersion in CaF_2 and CeO_2

Yi Wang, Lei A. Zhang, Shunli Shang, Zi-Kui Liu, and Long-Qing Chen
Materials Science and Engineering, The Pennsylvania State University, University Park, Pennsylvania 16802, USA
(Received 14 May 2013; published 18 July 2013)

We report the lattice dynamic properties of CaF_2 and CeO_2 obtained using a direct method in combination of a mixed-space approach accounting for the vibration-induced dipole-dipole interactions. We overcame the overestimation of T_{1u} TO mode shown in prior calculations using the linear response theory. For CaF_2, we employed the Perdew-Burke-Ernzerhof functional and achieved a significant improvement over previous linear response calculations by comparing the results with experimentally measured phonon dispersion curves. For CeO_2, we adopted the Heyd-Scuseria-Ernzerhof hybrid functional and an elongated supercell and obtained results in excellent agreement with experimental measurements. We attributed the improved calculation results to the convenience of the direct method in implementing new exchange-correlation functionals and use of the mixed-space approach for treating the long-range dipole-dipole interactions.

DOI: 10.1103/PhysRevB.88.024304 PACS number(s): 63.20.D−, 63.20.dk

A family of compounds, including XF_2 (X = Ca, Ba, Sr, Pb), XSi_2 (X = Mg, Sn, Ge, Pb), and XO_2 (X = Ce, Th, U, Pu), crystallizes in the face-centered cubic fluorite structure, wherein the cation is coordinated to eight anions, and each anion is surrounded by four cations. They showed unusually high anionic conductivity far below their melting points.[1] In particular, CaF_2 (Refs. 2,3) is a typical superionic conductor.[1] CeO_2 has been used in catalytic converters in automotive applications and as an electrolyte in fuel cells because of its relatively high oxygen ion conductivity.[4–7] CeO_2 is also interesting due to its electronic similarity to the nuclear materials of ThO_2, UO_2, and PuO_2.

Th paper is concerned with the accurate calculation of the lattice dynamics of CaF_2 and CeO_2. Our first objective is to resolve the existing disagreements between experimental measurements and previous calculations using the Vienna *Ab initio* Simulation Package (VASP), plane-wave self-consistent field (PWSCF), and ABINIT in the literature.[2–5,7–10] Our second objective is to compare the first-principles calculations of phonon frequencies from the direct approach[11–14] and from the linear response method.[15,16] Computationally, the advantage of the linear response method is that it directly evaluates the dynamical matrix through the density functional perturbation theory.[15,16] In comparison, the direct method is conceptually simple and straightforward to implement with a new potential or approximation, such as strong correlation,[17,18] the explicit treatment of the semicore electrons, the hybrid potential,[19,20] and particularly, the mixed-space approach.[13,14] The most appealing feature of the direct method is that the phonons at the nonzero exact wave vectors are calculated exactly with no further approximation.[21] Moreover, although it has generally been believed that it is difficult to handle the long-range dipole-dipole interactions in polar materials using the direct method,[11] our proposed mixed-space approach[13,14] has made it possible to determine accurately the lattice dynamics of polar materials within the direct approach.

Here, we briefly outline the mixed-space approach,[13,14] taking into account the vibration-induced dipole-dipole interactions. According to the reduced dynamical matrix from Wallace,[22] the reduced dynamical matrix at an arbitrary wave vector $\mathbf{q}$ is

$$\tilde{D}^{jk}_{\alpha\beta}(\mathbf{q}) = \frac{1}{\sqrt{\mu_j \mu_k}} \sum_{P}^{N} \phi^{jk}_{\alpha\beta}(0,P) \exp\{i\mathbf{q}\cdot[\mathbf{R}(P)-\mathbf{R}(0)]\} + f(\mathbf{q})\varphi^{jk}_{\alpha\beta}(\mathbf{q}), \quad (1)$$

where α and β represent the Cartesian axes, μ_j the atomic mass of the jth atom in the primitive unit cell, N the number of primitive unit cells in the supercell, $\mathbf{R}(P)$ the position of the Pth primitive unit cell in the supercell, and $\phi^{jk}_{\alpha\beta}(0,P)$ the real-space force constant between jth atom in the primitive cell 0 and kth atom in the primitive cell P. $\varphi^{jk}_{\alpha\beta}$ in Eq. (1) accounts for the contribution due to the vibration-induced dipole-dipole interactions and is given by

$$\varphi^{jk}_{\alpha\beta}(\mathbf{q}) = \frac{1}{\sqrt{\mu_j \mu_k}} \frac{4\pi}{NV} \frac{[\mathbf{q}\cdot\mathbf{Z}^*(j)]_\alpha\,[\mathbf{q}\cdot\mathbf{Z}^*(k)]_\beta}{\mathbf{q}\cdot\boldsymbol{\varepsilon}_\infty\cdot\mathbf{q}}, \quad (2)$$

where V is the volume of the primitive unit cell, $\mathbf{Z}^*(j)$ the Born effective charge tensor of the jth atom in the primitive unit cell, and $\boldsymbol{\varepsilon}_\infty$ the high-frequency static dielectric tensor, i.e., the contribution to the dielectric permittivity tensor from the electronic polarization.[15] The major result of the mixed-space approach[13,14] is the function of $f(\mathbf{q})$ in Eq. (1)

$$f(\mathbf{q}) = \sum_{P}^{N} \exp\{i\mathbf{q}\cdot[\mathbf{R}(P)-\mathbf{R}(0)]\}. \quad (3)$$

The physical significance of $f(\mathbf{q})$ is already discussed elsewhere.[13]

Here, we want to mention that the computational implementation of the above formulations is rather straightforward. Specifically for VASP, (version 5.2), the $\phi^{jk}_{\alpha\beta}(0,P)$ in Eq. (1) is simply the negative of the "SECOND DERIVATIVES" in the VASP OUTCAR output file. To consider the effect of the vibration-induced dipole-dipole interactions, the additional term is $f(\mathbf{q})\varphi^{jk}_{\alpha\beta}(\mathbf{q})$, where the value of $\varphi^{jk}_{\alpha\beta}(\mathbf{q})$ is solely dependent on $\mathbf{Z}^*(j)$ and $\boldsymbol{\varepsilon}_\infty$ which are readily available with VASP (5.x), noting that $f(\mathbf{q})$ is just a geometrical factor determined by the supercell shape and the $\mathbf{q}$ value. Therefore, Fourier-interpolation is still possible, and there is no need

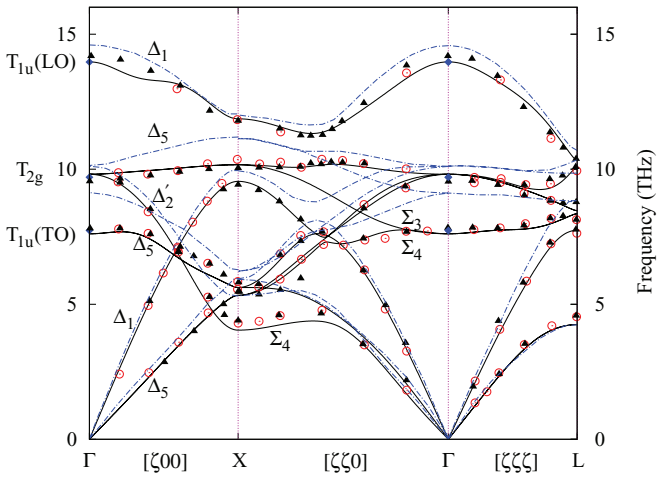

FIG. 1. (Color online) Phonon dispersions of CaF_2. The solid lines represent the present supercell calculation and the (blue) dot-dashed lines represent the previous linear response calculation by Verstraete and Gonze (Ref. 3). Open circles: neutron scattering data by Elcombe and Pryor (Ref. 30); solid triangles: neutron scattering data by Schmalzl *et al.* (Ref. 2); solid diamonds at the Γ point: Raman and infrared data (Refs. 31,32).

to separate $\phi^{jk}_{\alpha\beta}(0,P)$ into the short- and long-range parts because it was done previously.[16] The mixed-space approach, independently implemented by Zhao *et al.*[23] and Pang *et al.*,[24] is the default option of the phonopy package by Togo *et al.*[25] for handling vibration-induced dipole-dipole interactions.

Our phonon calculations of CaF_2 and CeO_2 are performed using the experimentally determined lattice parameters[3,7] and employing the projector-augmented wave (PAW) method[26,27] as implemented in the VASP package. For CaF_2, the Perdew-Burke-Ernzerhof (PBE)[28] exchange-correlation functional is chosen; the adopted pseudopotentials treat the Ca $3s^2 3p^6 4s^2$ and F $2s^2 2p^5$ shells as valence states; the 192-atom supercell in our phonon calculation is the $4 \times 4 \times 4$ superstructure of the primitive unit cell; the force constants are calculated using the Γ-centered $3 \times 3 \times 3$ k-mesh for the electronic Brillouin integration together with an energy cutoff 400 eV; and the Born effective charge and dielectric constant tensors are calculated following the linear response approach by Gajdoš *et al.*[29] with the Γ-centered $15 \times 15 \times 15$ k-mesh for the electronic Brillouin integration together with an energy cutoff 500 eV.

Figure 1 shows the comparisons among the calculated phonon dispersions of CaF_2 from the present PBE calculation and the previous linear response calculation by Verstraete and Gonze,[3] the neutron scattering data by Elcombe and Pryor,[30] the neutron scattering data by Schmalzl *et al.*,[2] and Raman and infrared data.[31,32] By comparison with experimental measurements, we see substantial improvement of the present direct calculation over the previous linear response calculations.

The primitive cell of a fluorite structure contains three nonequivalent atoms, corresponding to nine phonon modes in the dispersion relations, with three of them being the acoustic modes. At the Γ point, there are three distinct optic phonon modes based on group theory analysis, and their representations are a doubly degenerate infrared-active TO T_{1u}, a triply degenerate Raman-active mode T_{2g}, and an infrared-active nondegenerate LO T_{1u} in the order of increasing phonon frequency. From the Γ to the X point along the [100] direction, the T_{1u} (TO) mode is correlated to a doubly degenerate Δ_5 dispersion following the notation of Schmalzl *et al.*;[2] the T_{2g} mode is split into a doubly degenerate Δ_5 dispersion and a nondegenerate Δ_2' dispersion; and the T_{1u} (LO) mode is correlated to a nondegenerate Δ_1 dispersion. Meanwhile, from the Γ to the X point along the [110] direction, the T_{1u} (TO) mode is split into nondegenerate Σ_3 and Σ_4 dispersions following the notations of Weber *et al.*[33] and Elcombe and Pryor;[30] the T_{2g} mode is split into three nondegenerate Σ_1, Σ_2, and Σ_4 dispersions; and the T_{1u} (LO) mode is correlated to a nondegenerate Σ_1 dispersion.

For CaF_2, the differences in the calculated phonon dispersions using different exchange-correlation functionals have been analyzed by Schmalzl *et al.*[2] and by Verstraete and Gonze[3] using the linear response theory. Their calculated phonon dispersions agree with each other, but both show significantly higher frequency values for the T_{1u} TO mode at the Γ point, the Δ_5 dispersion starting from T_{1u} (TO) mode, the Δ_2' dispersion toward the X point that evolved into the Σ_4 acoustic dispersion along the [110] direction, and the Σ_3 and Σ_4 dispersions starting from T_{1u} (TO) mode.

For CeO_2, our main purpose is to demonstrate the accuracy of the Heyd-Scuseria-Ernzerhof (HSE) hybrid functional[19,20] compared to the existing VASP calculations[4,5,8,10] and linear response calculation using ABINIT.[7] We chose the pseudopotentials that treat the Ce $5s^2 5p^6 6s^2 5d^1 4f^1$ and O $2s^2 2p^4$ shells as valence states. For the HSE calculation, the $4 \times 4 \times 4$ supercell is still computationally prohibitive. As an alternative, we adopt elongated supercells with lengths along the [100], [110], and [111] directions being $\sqrt{1/2}a \times \sqrt{1/2}a \times 4a$, $\sqrt{1/2}a \times a \times 2\sqrt{2}a$, and $\sqrt{1/2}a \times \sqrt{3/2}a \times 4a$, respectively, where $a = 5.411$ is the experimental lattice constant.[34] These three supercells contain 24, 24, and 36 atoms and lead to 8, 8, and 6 exact $\mathbf{q}$ points along the [100], [110], and [111] directions. The force constants are calculated using the Γ-centered $5 \times 5 \times 1$ k-mesh for the electronic Brillouin integration together with an energy cutoff 400 eV. The Born effective charge and dielectric constant tensors are calculated following the Berry-phase approach by Nunes and Gonze,[35] with the Γ-centered $15 \times 15 \times 15$ k-mesh for the electronic Brillouin integration with an energy cutoff 500 eV.

Figure 2 shows the comparisons among the calculated phonon dispersions of CeO_2 from the present HSE calculation and the previous linear response calculation by Gürel and Eryiğit,[7] the neutron scattering data by Clausen *et al.*,[36] and the Raman and infrared data.[37] We believe that the best calculated phonon dispersions in the literature are those by Gürel and Eryiğit.[7] Our calculated phonon dispersions show significant improvements over the previous calculations for CeO_2 using VASP in the literature.[4,5,7–10] The moderate disagreement at the X point between the dispersions along [100] and [110] directions are due to numerical uncertainties, possibly due to the mismatches between the two directions of the employed k-meshes for the electronic Brillouin integration.

In terms of the neutron scattering data of CeO_2 by Clausen *et al.*,[36] the overall improvement of the present HSE calculation over the linear response calculation by Gürel and Eryiğit[7] is not as clear as the case of CaF_2. Nevertheless, when approaching

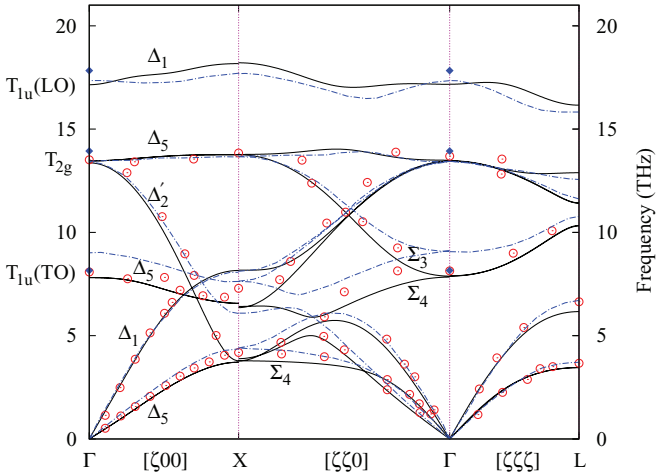

FIG. 2. (Color online) Phonon dispersions of CeO_2. The solid lines represent the present supercell calculation and the (blue) dot-dashed lines represent the previous linear response calculation by Gürel and Eryiğit (Ref. 7). Open circles: neutron scattering data by Clausen *et al*. (Ref. 36); solid diamonds at the Γ point: Raman and infrared data (Ref. 37).

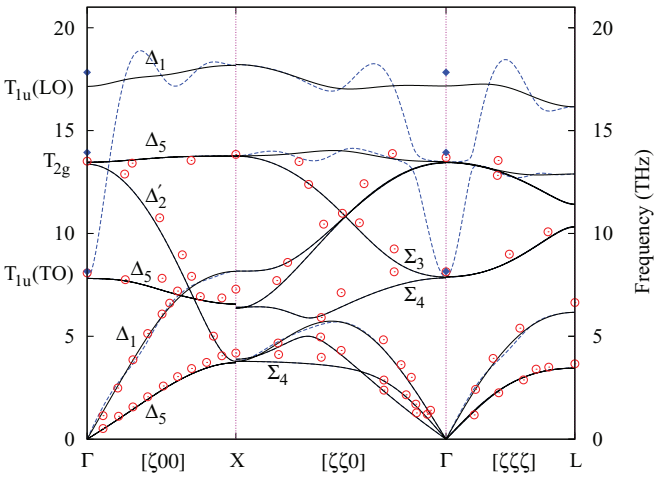

FIG. 3. (Color online) Comparison of the calculation phonon dispersions of CeO_2 with (solid lines) and without (dashed lines) considering the vibration-induced dipole-dipole interaction. The other symbols have the same meanings as Fig. 2.

the X point along the [100] direction, we do see an improved agreement for the Δ_2' dispersion, which evolved into the Σ_4 acoustic dispersion along the [110] direction. In particular at the X point, the calculation of Gürel and Eryiğit[7] gave a frequency of ∼6.2 THz for the Δ_2' dispersion; the present HSE calculation gives a phonon frequency of 3.79 THz, which is almost the same as the calculated phonon frequency of 3.72 THz of the acoustic phonon Δ_5 dispersion at the X point, being in good agreement with the value of ∼4.2 THz evaluated by Clausen *et al*. based on their neutron scattering data. Note that the fitting of Clausen *et al*. also shows that the Δ_2' dispersion is almost degenerate with the acoustic phonon Δ_5 dispersion at the X point. Additionally, Gürel and Eryiğit[7] gave higher phonon frequency for the T_{1u} (TO) mode at the Γ point than the neutron scattering data of Clausen *et al*.,[36] resulting in higher phonon frequency data than the neutron scattering measurement for the whole Δ_5 dispersion starting from the T_{1u} (TO) mode. The calculated phonon dispersions of CeO_2 by Gupta *et al*.[9] using PWSCF were rather inaccurate, particularly along the [110] direction, perhaps due to their use of the ultrasoft pseudopotentials.

For the calculations of the phonon dispersions of CeO_2 employing the direct method, a specific issue to be mentioned here is concerned with the previously published calculations employing Parliński's approach.[12] For example, Xiao *et al*.[8] reported the calculated results within the local-density approximation (LDA) to the exchange-correlation functional; Shi *et al*.[4] and Li *et al*.[10] reported results employing LDA + U; and Sevik and Cagin[5] examined the U effects on the calculated phonon dispersion. These works overlooked the issue of the deficiency of Parliński's approach[38] in taking into account the vibration-induced dipole-dipole interactions. While Parliński's method is the best approach to date for calculating phonon frequencies of nonpolar materials within the direct method (namely, small displacement method or supercell approach), the reply of Parliński *et al*.[38] to the comment of Detraux *et al*.[39] did not properly take into account the dipole-dipole interactions properly. In particular, to account for the vibration-induced dipole-dipole interaction, Parliński *et al*.[38] applied a free parameter ρ in the form of Gaussian smearing

$$f_{PLK}(\rho,\mathbf{q}) = \exp(-\mathbf{q}^2/\rho^2) \tag{4}$$

to the Cochran and Cowley formula[40] at the limit of $\mathbf{q} \to 0$. Unfortunately, almost none of the previous publications (e.g. Refs. 4,5, and 41–55) except the original reply by Parliński *et al*.[38] mentioned the empirical parameter ρ. Furthermore, Eq. (4) results in a nonzero correction at the nonzero exact wave-vector points, in contradiction to the theorem[11,13,14,56] that at the nonzero exact wave-vector points, the phonon frequencies calculated within the direct method are exact, i.e., no nonanalytical correction terms are needed at the nonzero exact wave-vector points.

We would also like to point out that the effect of vibration-induced dipole-dipole interaction on phonon frequencies is not limited to the vicinity of $\mathbf{q} \to 0$, as it is commonly believed. Figure 3 shows the comparison of the calculated phonon dispersions of CeO_2 with and without considering the vibration-induced dipole-dipole interactions. The salient feature of the mixed-space approach is best seen by the intersections between the calculated dispersion curves without [dashed line in Fig. 3 starting from the T_{1u} (TO) mode at the Γ point] and those with [solid line in Fig. 3 starting from the T_{1u} (LO) mode at the Γ point] the vibration-induced dipole-dipole interactions. Note from Fig. 3 that the numbers of intersections between the solid curve [i.e., the curve starting from the T_{1u} (LO) mode] and the dashed curve are 4, 4, and 3, respectively, along the [100], [110], and [111] directions, indicating the exact wave-vector points within half of the Brillouin starting from the zone center toward the zone boundaries. The intersections imply that at the nonzero exact wave-vector points, the effects of the vibration-induced dipole-dipole interactions on phonon frequencies are zero.

For completeness, Table I gives a summary of the high-frequency dielectric constant, Born effective charge of the cation, and the zone-center phonon frequencies for CaF_2 and

TABLE I. High-frequency dielectric constant ε_∞, Born effective charge of cation Z^*, and zone-center phonon frequencies (cm^{-1}) for CaF_2 and CeO_2.

	ε_∞	Z^*	$Z^*/\sqrt{\varepsilon_\infty}$	$\omega_{T_{1u}}$(TO)	$\omega_{T_{2g}}$	$\omega_{T_{1u}}$(LO)
–	–	–	CaF_2		–	–
PBE[a]	2.270	2.370	1.573	253	327	466
TM-GGA[b]	2.02	2.18	1.53	305	338	487
Expt.[c]	2.045	–	–	257	322	463
–	–	–	CeO_2	–	–	–
HSE[a]	5.696	5.558	2.329	264	451	573
HGH-LDA[d]	6.23	5.576	2.234	301	450	579
Expt.[e]	5.31	–	–	272	465	595

[a]This work.
[b]ABINIT linear response calculation within the generalized gradient approximation (GGA) using Troullier-Martins pseudopotentials by Verstraete and Gonze.[3]
[c]Raman and infrared data.[31,32]
[d]ABINIT linear response calculation within LDA using Hartwigsen-Goedecker-Hutter pseudopotentials by Gürel and Eryiğit.[7]
[e]Raman and infrared data.[37]

CeO_2 calculated by the present work, and the best experimental or theoretical results in the literature.[3,7,31,32,37]

In conclusion, we calculated the lattice dynamics of CaF_2 using the PBE functional and CeO_2 using the HSE hybrid functional. The comparison with experiments shows significant improvements over the previous direct calculations employing VASP as well as linear response calculations employing PWSCF or ABINIT. The mixed-space approach leads to more accurate phonon dispersion curves than Parliński's approach[38] in handling the vibration-induced dipole-dipole interactions. We achieved the improvements with new exchange-correlation functionals in the direct method and the mixed-space approach.

This work was supported by the US Department of Energy, Office of Basic Energy Sciences, Division of Materials Sciences and Engineering under Award No. DE-FG02-07ER46417, by the National Energy Technology Laboratory (Grant No. 2010-SC-RES-30033026 and the RES Contract No. DE-FE00400 in Turbines), and by the National Science Foundation (NSF) through Grant No. CHE-1230924. First-principles calculations were conducted at the National Energy Research Scientific Computing Center, which is supported by the Office of Science of the US Department of Energy under Contract No. DE-AC02-05CH11231 and the Penn State LION Clusters funded by the NSF through Grant No. OCI-0821527.

[1]M. J. Gillan, J. Phys. C **19**, 3517 (1986).
[2]K. Schmalzl, D. Strauch, and H. Schober, Phys. Rev. B **68**, 144301 (2003).
[3]M. Verstraete and X. Gonze, Phys. Rev. B **68**, 195123 (2003).
[4]S. Q. Shi, X. Z. Ke, C. Y. Ouyang, H. Zhang, H. C. Ding, Y. H. Tang, W. W. Zhou, P. J. Li, M. S. Lei, and W. H. Tang, J. Power Sources **194**, 830 (2009).
[5]C. Sevik and T. Cagin, Phys. Rev. B **80**, 014108 (2009).
[6]J. L. F. Da Silva, M. V. Ganduglia-Pirovano, J. Sauer, V. Bayer, and G. Kresse, Phys. Rev. B **75**, 045121 (2007).
[7]T. Gürel and R. Eryiğit, Phys. Rev. B **74**, 014302 (2006).
[8]H. Y. Xiao, Y. Zhang, and W. J. Weber, Acta Mater. **61**, 467 (2013).
[9]A. Gupta, A. Kumar, M. S. Hegde, and U. V. Waghmare, J. Chem. Phys. **132**, 194702 (2010).
[10]P. J. Li, W. W. Zhou, Y. H. Tang, H. Zhang, and S. Q. Shi, Acta Phys. Sin. **59**, 3426 (2010).
[11]D. Alfe, Comput. Phys. Commun. **180**, 2622 (2009).
[12]K. Parlinski, Z.-Q. Li, and Y. Kawazoe, Phys. Rev. Lett. **78**, 4063 (1997).
[13]Y. Wang, S. L. Shang, Z. K. Liu, and L. Q. Chen, Phys. Rev. B **85**, 224303 (2012).
[14]Y. Wang, J. J. Wang, W. Y. Wang, Z. G. Mei, S. L. Shang, L. Q. Chen, and Z. K. Liu, J. Phys.: Condens. Matter **22**, 202201 (2010).
[15]S. Baroni, S. de Gironcoli, A. Dal Corso, and P. Giannozzi, Rev. Mod. Phys. **73**, 515 (2001).
[16]X. Gonze and C. Lee, Phys. Rev. B **55**, 10355 (1997).
[17]Y. Wang, J. E. Saal, J. J. Wang, A. Saengdeejing, S. L. Shang, L. Q. Chen, and Z. K. Liu, Phys. Rev. B **82**, 081104 (2010).
[18]A. Floris, S. de Gironcoli, E. K. U. Gross, and M. Cococcioni, Phys. Rev. B **84**, 161102 (2011).
[19]J. Heyd, G. E. Scuseria, and M. Ernzerhof, J. Chem. Phys. **118**, 8207 (2003).
[20]J. Heyd, G. E. Scuseria, and M. Ernzerhof, J. Chem. Phys. **124**, 219906 (2006).
[21]G. Kern, G. Kresse, and J. Hafner, Phys. Rev. B **59**, 8551 (1999).
[22]D. C. Wallace, *Thermodynamics of Crystals* (Wiley, New York, 1972).
[23]Y. Zhao, K. T. E. Chua, C. K. Gan, J. Zhang, B. Peng, Z. Peng, and Q. Xiong, Phys. Rev. B **84**, 205330 (2011).
[24]J. W. L. Pang, W. J. L. Buyers, A. Chernatynskiy, M. D. Lumsden, B. C. Larson, and S. R. Phillpot, Phys. Rev. Lett. **110**, 157401 (2013).
[25]A. Togo, F. Oba, and I. Tanaka, Phys. Rev. B **78**, 134106 (2008).
[26]P. E. Blöchl, Phys. Rev. B **50**, 17953 (1994).
[27]G. Kresse and D. Joubert, Phys. Rev. B **59**, 1758 (1999).
[28]J. P. Perdew, K. Burke, and M. Ernzerhof, Phys. Rev. Lett. **77**, 3865 (1996).
[29]M. Gajdoš, K. Hummer, G. Kresse, J. Furthmuller, and F. Bechstedt, Phys. Rev. B **73**, 045112 (2006).
[30]M. M. Elcombe and A. W. Pryor, J. Phys. C **3**, 492 (1970).
[31]W. Kaiser, W. G. Spitzer, L. E. Howarth, and R. H. Kaiser, Phys. Rev. **127**, 1950 (1962).
[32]J. P. Russell, Proc. Phys. Soc. London **85**, 194 (1965).
[33]W. H. Weber, K. C. Hass, and J. R. McBride, Phys. Rev. B **48**, 178 (1993).
[34]L. Gerward, J. S. Olsen, L. Petit, G. Vaitheeswaran, V. Kanchana, and A. Svane, J. Alloys Compd. **400**, 56 (2005).
[35]R. W. Nunes and X. Gonze, Phys. Rev. B **63**, 155107 (2001).
[36]K. Clausen, W. Hayes, J. E. Macdonald, R. Osborn, P. G. Schnabel, M. T. Hutchings, and A. Magerl, J. Chem. Soc., Faraday Trans. 2 **83**, 1109 (1987).

[37]S. Mochizuki, Phys. Status Solidi B **114**, 189 (1982).
[38]K. Parliński, Z. Q. Li, and Y. Kawazoe, Phys. Rev. Lett. **81**, 3298 (1998).
[39]F. Detraux, P. Ghosez, and X. Gonze, Phys. Rev. Lett. **81**, 3297 (1998).
[40]W. Cochran and R. A. Cowley, J. Phys. Chem. Solids **23**, 447 (1962).
[41]Z. Lodziana and K. Parliński, Phys. Rev. B **67**, 174106 (2003).
[42]L. G. Hector, Jr., J. F. Herbst, W. Wolf, P. Saxe, and G. Kresse, Phys. Rev. B **76**, 014121 (2007).
[43]C. H. Hu, A. R. Oganov, Y. M. Wang, H. Y. Zhou, A. Lyakhov, and J. Hafner, J. Chem. Phys. **129**, 234105 (2008).
[44]U. D. Wdowik and K. Parliński, Phys. Rev. B **78**, 224114 (2008).
[45]M. Derzsi, P. Piekarz, P. T. Jochym, J. Lazewski, M. Sternik, A. M. Oles, and K. Parlinski, Phys. Rev. B **79**, 205105 (2009).
[46]Y. H. Duan and D. C. Sorescu, Phys. Rev. B **79**, 014301 (2009).
[47]R. A. Evarestov and M. V. Losev, J. Comput. Chem. **30**, 2645 (2009).
[48]C. Jiang, C. R. Stanek, N. A. Marks, K. E. Sickafus, and B. P. Uberuaga, Phys. Rev. B **79**, 132110 (2009).
[49]X. H. Luo, W. Zhou, S. V. Ushakov, A. Navrotsky, and A. A. Demkov, Phys. Rev. B **80**, 134119 (2009).
[50]S. Minamoto, M. Kato, K. Konashi, and Y. Kawazoe, J. Nucl. Mater. **385**, 18 (2009).
[51]S. Q. Shi, H. Zhang, X. Z. Ke, C. Y. Ouyang, M. S. Lei, and L. Q. Chen, Phys. Lett. A **373**, 4096 (2009).
[52]U. D. Wdowik and D. Legut, J. Phys.: Condens. Matter **21**, 275402 (2009).
[53]U. D. Wdowik and K. Parliński, J. Phys.: Condens. Matter **21**, 125601 (2009).
[54]J. Wrobel, K. J. Kurzydlowski, K. Hummer, G. Kresse, and J. Piechota, Phys. Rev. B **80**, 155124 (2009).
[55]U. D. Wdowik, J. Phys.: Condens. Matter **22**, 045404 (2010).
[56]G. Kern, G. Kresse, and J. Hafner, Phys. Rev. B **59**, 8551 (1999).